



Published in final edited form as:

Nature. 2009 February 19; 457(7232): 981–989. doi:10.1038/nature07767.

## N-APP binds DR6 to cause axon pruning and neuron death via distinct caspases

Anatoly Nikolaev<sup>1</sup>, Todd McLaughlin<sup>2</sup>, Dennis O’Leary<sup>2</sup>, and Marc Tessier-Lavigne<sup>1,3</sup>

<sup>1</sup> Division of Research, Genentech, Inc, 1 DNA Way, South San Francisco, CA, 94080

<sup>2</sup> Molecular Neurobiology Laboratory, The Salk Institute, 10010 North Torrey Pines Road, La Jolla, CA 92037, USA

### Abstract

Naturally-occurring axonal pruning and neuronal cell death help sculpt neuronal connections during development, but their mechanistic basis remains poorly understood. We report that Amyloid Precursor Protein (APP) and Death Receptor 6 (DR6) activate a widespread caspase-dependent self-destruction program. DR6 is broadly expressed by developing neurons, and is required for normal cell body death and axonal pruning both *in vivo* and after trophic factor deprivation *in vitro*. Unlike neuronal cell body apoptosis, which requires caspase-3, we show that axonal degeneration requires caspase-6, which is activated in a punctate pattern that parallels the pattern of axonal fragmentation. DR6 is activated locally by an inactive surface ligand(s) that is released in active form upon trophic factor deprivation, and we identify APP as a DR6 ligand. Trophic factor deprivation triggers shedding of surface APP in a beta-secretase (BACE)-dependent manner. Loss- and gain-of-function studies support a model in which a cleaved amino-terminal fragment of APP (N-APP) binds DR6 and triggers degeneration. Genetic support is provided by a common neuromuscular junction phenotype in mutant mice. Our results indicate that APP and DR6 are components of a neuronal self-destruction pathway, and suggest that an extracellular fragment of APP, acting via DR6 and caspase-6, contributes to Alzheimer’s disease.

### Introduction

The initial formative phase of nervous system development, involving generation of neurons and extension of axons, is followed by a regressive phase in which inappropriate axonal branches are pruned to refine connections, and many neurons are culled to match the numbers of neurons and target cells<sup>1–3</sup>. Loss of neurons and branches also occurs in the adult after injury, and underlies the pathophysiology of many neurodegenerative diseases<sup>1,4</sup>.

Our understanding of regressive events in development remains fragmentary. Degeneration can result “passively” from loss of support from trophic factors like Nerve Growth Factor (NGF)<sup>1–3</sup>. There is also evidence for “active” mechanisms in which extrinsic signals trigger degeneration via proapoptotic receptors, including some members of the Tumor Necrosis Factor (TNF) receptor superfamily like p75NTR, Fas, and TNFR1 (Fig. 1a)<sup>5</sup>. However, the full complement of degeneration triggers remains incompletely understood.

<sup>3</sup>Author for manuscript correspondence: Marc Tessier-Lavigne, Tel: 650 225 1175, Fax: 650 225 4000, Email: E-mail: marctl@gene.com. Reprints and permissions information is available at [npgnature.com/reprintsandpermissions](http://npgnature.com/reprintsandpermissions).

A.N. and M.T.L. declare competing financial interests.

Our understanding of intracellular mechanisms of neuronal dismantling is also incomplete. It is well documented that developmental neuronal cell body degeneration requires the apoptotic effectors Bax and caspase-3<sup>6–8</sup>; pruning of a particular dendrite in *Drosophila* is also caspase-dependent<sup>9,10</sup>. Developmental axonal degeneration likewise has many hallmarks of apoptosis, including blebbing, fragmentation, and phagocytic clearing of debris by neighboring cells<sup>2,4</sup>. However, it has been argued that axonal degeneration is caspase-independent, because caspase-3 inhibitors block cell body but not axonal degeneration<sup>8</sup> (reflecting higher activation of caspase-3 in cell bodies compared to axons<sup>11</sup>) and because genetic manipulations to inhibit apoptosis did not block axonal degeneration in some models<sup>12,13</sup>. These results suggested the existence of a caspase-independent program of axonal degeneration<sup>1,2,4</sup>, but its molecular nature has remained elusive.

While studying expression of all TNF receptor superfamily members<sup>14</sup>, we found that DR6 (a.k.a. TNF receptor superfamily member 21 (TNFRSF21)), one of eight members possessing a cytoplasmic Death Domain (Fig 1a), is widely expressed by neurons as they differentiate and become pro-apoptotic. DR6 is an orphan receptor<sup>15</sup>. In transfected cells, it triggers cell death in a Jun N-terminal kinase-dependent manner<sup>16</sup>. *In vivo*, it regulates lymphocyte development<sup>17,18</sup>, but its involvement in neural development is unknown.

Here we show that DR6 links passive and active degeneration mechanisms. Following trophic deprivation, DR6 triggers neuronal cell body and axon degeneration. Because DR6 signals via Bax and caspase-3 in cell bodies, we revisited caspase involvement in axonal degeneration, and found that axonal degeneration indeed requires both Bax and a distinct effector, caspase-6. Our results also indicated that DR6 is activated by a prodegenerative ligand(s) that is surface-tethered but released in active form upon trophic deprivation. In searching for candidate ligands with these properties, we considered APP, a transmembrane protein that undergoes regulated shedding and is causally implicated in Alzheimer's disease<sup>19–22</sup>, because we had previously found it to be highly expressed by developing neurons and especially axons (see Fig. 4h); since Alzheimer's is marked by neuron and axon degeneration, we had therefore long wondered whether it participates in developmental degeneration. We show that an extracellular fragment of APP is indeed a ligand for DR6 – as is a fragment of its close relative, APLP2 – that triggers degeneration of cell bodies via caspase-3 and axons via caspase-6, and we propose that this developmental mechanism is hijacked in Alzheimer's disease.

## Results

### DR6 regulates neuronal death *in vitro* and *in vivo*

To explore involvement of the TNFR superfamily in neural development, we screened its 28 members by *in situ* hybridization in midgestation mouse embryos. We came to focus on DR6 (Fig. 1a), because its mRNA is expressed at low levels in proliferating progenitors in the spinal cord, but highly expressed by differentiating neurons within the spinal cord and adjacent dorsal root ganglia (DRG) (Fig. 1b).

Because *DR6*-expressing neurons are proapoptotic at these stages, we examined whether DR6 regulates neuronal death following trophic factor deprivation *in vitro*, focusing on three sets of spinal neurons: commissural, motor, and sensory (Supplementary Fig. 1a). Initially, we found that siRNA knock-down of *DR6* protected commissural neurons from degeneration (Supplementary Fig. 2). This prompted us to screen monoclonal antibodies to DR6 for their ability to mimic this protection; we selected antibody 3F4 (anti-DR6.1). When embryonic day (E) 11.5 mouse dorsal spinal cord explants are cultured for 24hr, commissural cell bodies and axons are healthy, but when cultured 24hr longer they degenerate<sup>23</sup>; anti-DR6.1 inhibited this degeneration (Fig. 1c, f), mimicking *DR6* knock-down. Anti-DR6.1 also protected sensory neurons from E12.5 DRGs cultured for 48hr with NGF, and motoneurons from E12.5 ventral

spinal cord explants cultured for 24hr with Brain-derived Neurotrophic Factor (BDNF) and Neurotrophin-3 (NT3): when these cultures were deprived of trophic factor and cultured 24hr longer, they showed massive cell death and axonal degeneration, which were largely inhibited by anti-DR6.1 (Fig. 1d–f; Supplementary Fig. 1b). Similar protection was observed when DRGs or ventral explants from a *DR6* null mutant<sup>17</sup> were deprived in absence of anti-DR6.1 (Supplementary Fig. 4b, and not shown), confirming that anti-DR6.1 is function-blocking. DR6 inhibition (by antibody, siRNA, or genetic deletion) caused a delay rather than complete block, since more degeneration was observed in each case 24–48hr later (Fig. 2b, Supplementary Fig. 4b, and not shown).

We next examined DR6 function in cell death *in vivo*. Extensive neuronal apoptosis, visualized by expression of activated caspase-3, occurs in spinal cord and DRG between E12.5 and E15.5 (Fig. 1g). In the *DR6* mutant, there was a ~50% reduction in number of apoptotic neurons (Fig. 1g, h). This correlated with a higher motoneuron number at E14.5, but the number returned to wild-type level by E18 (Supplementary Fig. 3), after the cell death period. Thus, antagonizing DR6 delays death of multiple neuronal populations *in vitro* and *in vivo*.

### DR6 regulates axonal pruning *In vitro* and *in vivo*

DR6 protein is expressed not just by cell bodies (not shown) but also axons (Supplementary Fig. 4a). Protection of axons by DR6 inhibition might therefore reflect a direct role for DR6 in axons. To explore this, we used compartmented (“Campenot”) chambers<sup>24</sup> (Fig. 2a). Sensory neurons are placed in a central chamber containing NGF; their axons grow under a partition into NGF-containing side-chambers. Fluid exchange between chambers is limited, so NGF deprivation in a side-chamber elicits local axon degeneration while sparing cell bodies<sup>24</sup>. Locally-deprived axons degenerate in a stereotyped manner, with initial signs by 6 hr and extensive degeneration by 12–24hr, but when anti-DR6.1 was added to the deprived side-chamber, degeneration was blocked at 24hr and still largely impaired at 48hr (Fig. 2b, c; a similar delay was observed when axons of neurons from *DR6* knock-out mice were locally deprived (Supplementary Fig. 4b, c)). Thus, DR6 functions in axons to trigger degeneration.

To determine whether DR6 functions in axonal pruning *in vivo*, we studied the well-characterized retino-collicular projection, which develops from an initially exuberant projection of retinal ganglion cell (RGC) axons to a focused termination zone (TZ) in the superior colliculus (SC). Temporal RGC axons initially extend into posterior SC, well past their future TZ in anterior SC (Supplementary Fig. 5a). This diffuse projection is then refined by axonal degeneration<sup>2</sup>, such that by postnatal day (P) 6 in wild-type mice few axon segments persist in areas beyond the TZ, as revealed by focal injection of DiI into temporal retina (Fig. 2c, d; Supplementary Fig. 2a, b). In contrast, in P6 *DR6* mutant mice, many more RGC axons and arbors are present in areas far from the TZ (Fig. 2e, f; Supplementary Fig. 5c, d, d’): we found an 83% increase in axon-positive domains within 400µm of the TZ (Supplementary Fig. 5e, e’) in *DR6* *-/-* (n=7) compared to wild-type mice (n=7;  $p < 0.05$ , Student’s t-test). The defect at P6 represents a delay in pruning, not a complete block, as assessed by examining labeled axons at P4, P5, P6 and P9: at each age, the mutant has more extraneous axons than the wild-type, and fewer are observed in both wild-type and mutant at each age compared to earlier time points, but by P9 the mutant and wild type projections are indistinguishable (not shown). Thus, blocking DR6 function delays pruning of sensory axons *in vitro* and retinocollicular axons *in vivo*.

### Axonal degeneration requires caspase-6 function

Since DR6 regulates both cell body apoptosis and axonal degeneration, we revisited whether an apoptotic pathway is also involved in axons. In support, we found that Bax, an effector in the intrinsic apoptotic pathway, is required in axons, since local sensory axon degeneration in

Campanot chambers was blocked by genetic deletion of *Bax* (Fig. 3a) or by local addition of a Bax inhibitor (e.g. Supplementary Fig. 9b). Consistent with evidence that caspase-3 mediates cell body but not axon degeneration<sup>8,11</sup>, we found that pro-caspase-3 is highly enriched in cell bodies (Fig. 3b, Supplementary Fig. 6a) and that zDEVD-fmk, an inhibitor of effector caspases 3 and 7, blocked cell body but not axon degeneration (Fig. 3c, c'; Supplementary Fig. 6b, c). There is, however, a third effector caspase, caspase-6. We found that pro-caspase-6 is expressed in both cell bodies and axons and that the caspase-6 inhibitor zVEID-fmk blocked degeneration of sensory, motor and commissural axons (Figures 3b, c, c'; Supplementary Fig. 6a–c), suggesting that caspase-6 regulates axonal degeneration. We verified these results using RNA interference in sensory and commissural neurons: *caspase-3* knock-down protected cell bodies significantly but had only a minor protective effect on axons, whereas *caspase-6* knock-down protected axons significantly with only minor effect on cell bodies (Fig. 3d, d'). Thus, distinct caspases mediate cell body and axon degeneration.

To visualize caspase activation, we first used the fluorescent reporters FAM-DEVD-fmk (for caspase-3/7) and FAM-VEID-fmk (for caspase-6), which bind covalently to activated target caspases. In NGF-deprived sensory neurons, the caspase-3/7 reporter labeled cell bodies but not axons, consistent with a prior study<sup>11</sup>; in contrast, caspase-6 reporter labeling was observed in both cell bodies and axons, and axonal labeling occurred in regularly-spaced “puncta”, giving a “beads on a string” appearance (Supplementary Fig. 6f). To control for reporter specificity, we used a selective antibody to cleaved caspase-6 and observed a similar punctate pattern in axons (Fig. 3e, f), whereas antibodies to cleaved caspase-3 only label cell bodies (Fig. 1c; ref. (11)). Caspase-6 activation was confirmed biochemically (Supplementary Fig. 6e). Interestingly, caspase-6 activation appeared at sites of microtubule fragmentation (assessed by loss of tubulin immunoreactivity) (Fig. 3e, f), suggesting that caspase-6 activation drives microtubule destabilization. Punctate caspase-6 activation was dramatically reduced by anti-DR6.1 (Fig. 3e) and abolished in *Bax*<sup>-/-</sup> neurons (not shown), suggesting that caspase-6 acts downstream of Bax in the pathway triggered by DR6. However, the possibility of feedback loops in apoptotic pathways makes this interpretation tentative.

### A DR6 ligand(s) on neurons is shed in response to trophic deprivation

Since DR6 is a receptor-like protein, we asked whether it is activated by a ligand(s). If so, the DR6 ectodomain might be capable of binding the ligand(s) and blocking its action (Fig. 4a). Consistent with this, the DR6 ectodomain fused to human Fc (DR6-Fc) mimicked anti-DR6.1 in delaying degeneration (Fig. 4a–c; Supplementary Figs. 7a and 13). To search for DR6 binding sites on axons and in conditioned medium, we used the DR6 ectodomain fused to alkaline phosphatase (DR6-AP), which can be visualized by AP histochemistry. Purple AP reaction product was observed on sensory and motor axons cultured with trophic factors when they were preincubated with DR6-AP but not AP alone, but binding was dramatically reduced following trophic deprivation (Supplementary Fig. 7b, c). To control for loss of axonal membrane, we blocked degeneration with a Bax inhibitor (not shown) or using neurons from *Bax*<sup>-/-</sup> mice (Fig. 4d) and observed even greater reduction in DR6-AP binding (residual binding seen without Bax inhibition might reflect non-specific binding to degenerating axons). To determine whether DR6-binding sites were shed, we harvested medium conditioned by sensory axons (in Campanot chambers) or motoneurons (in explant culture) (a Bax inhibitor was added to block non-specific release from degeneration). Proteins were separated on non-reducing gels, blotted to nitrocellulose, and probed with DR6-AP. Little signal was seen in medium conditioned by either neuronal type in presence of trophic factor. However, 48hr after trophic deprivation, DR6-AP bound a prominent band around ~35 kDa and a minor band around ~100 kDa in both cultures (Fig. 4e). Together, these results support a “Ligand Activation” model in which a prodegenerative DR6 ligand(s) is present on the neuronal surface

and inactive, but shed into medium in active form following trophic deprivation (Fig. 4f), allowing it to bind and activate DR6.

### The amino terminus of APP is a regulated DR6 ligand

Several properties of APP made it a candidate for a DR6 ligand: (i) it is highly expressed by developing spinal and sensory neurons and their axons (Fig. 4g); (ii) its ectodomain can be shed in a regulated fashion<sup>19,20</sup>; and (3) it is tied to degeneration through its links to Alzheimer's disease<sup>19–22</sup>. In an initial experiment, we found that DR6-AP bound APP expressed in COS cells (Supplementary Fig. 8a). This prompted us to test whether the bands detected by DR6-AP in conditioned medium (Fig. 4e) represent APP ectodomain fragments. APP is cleaved by alpha-secretases or beta-secretases (including, in neurons, BACE1<sup>25</sup>) at distinct sites in its juxtamembrane region (Fig. 4h) to release ~100 kDa ectodomain fragments termed, respectively, sAPP $\alpha$  or sAPP $\beta$ <sup>19,20</sup>. We probed conditioned medium with a polyclonal antibody to the APP amino terminus (anti-N-APP(poly), which also binds the APP relative APLP2: see below) and an antibody selective for the carboxy terminal epitope of sAPP $\beta$  exposed by BACE cleavage (anti-sAPP $\beta$ ) (Fig. 4h). Remarkably, anti-N-APP(poly) detected bands similar to those detected by DR6-AP: major at ~35 kDa and minor at ~100kDa, both highly enriched after trophic deprivation (Fig. 4i); anti-sAPP $\beta$  detected a minor ~100 kDa band and a major band at ~55 kDa (Fig. 4j), also both enriched after trophic deprivation. These results suggest that trophic deprivation triggers BACE cleavage of APP to yield the ~100 kDa sAPP $\beta$  (detected by both antibodies), which undergoes an additional cleavage(s) to yield a ~55 kDa carboxy-terminal fragment (detected by anti-sAPP $\beta$ ) and an amino-terminal ~35 kDa fragment (detected by anti-N-APP(poly)), which we term N-APP. The site of additional cleavage(s) is unknown, but based on fragment sizes is expected to be around the junction between the APP “acidic” and “E2” domains (amino acid 286); indeed, recombinant APP[1–286] ran at ~35 kDa and was detected with anti-N-APP(poly) (Fig. 4j), similar to N-APP.

Supporting cleavage of APP by BACE, we found that APP expression on the surface cultured sensory and motor axons, as assessed with anti-N-APP(poly) and with antibody 4G8 to the APP juxtamembrane region (Fig. 4h), is high in presence of trophic factor but lost after trophic deprivation, and that surface loss is blocked by three structurally divergent BACE inhibitors (OM99-2, BACE inhibitor IV, and the highly selective AZ-29<sup>26</sup>) but not the alpha-secretase inhibitor TAPI (Fig 4k; Supplementary Figs. 9a–c, and 10a; and not shown). Interestingly, 4G8 partially inhibited surface loss (Supplementary Fig. 9d), presumably through steric hindrance of BACE. Loss of surface APP occurred progressively and in “patches”, with little lost at 3 hrs, more at 6–12hrs, and most by 24hr (Fig. 4k; Supplementary Fig. 10b; and not shown). Total APP visualized after permeabilization did not change detectably (Supplementary Fig. 10b). Surface loss was not affected by Bax or caspase-6 inhibitors, or in neurons from *Bax*<sup>-/-</sup> mice (Fig 4k; Supplementary Figs. 9c, 10c).

The striking similarity of bands detected by anti-N-APP(poly) and DR6-AP suggested that DR6 binds N-APP. Indeed, depletion of conditioned medium with anti-N-APP(poly) eliminated DR6-AP binding sites (Fig. 4i), and purified DR6-Fc bound purified recombinant APP[1–286] in pull-down (Fig. 4j) and ELISA (Supplementary Fig. 8c) assays. The interaction detected by ELISA is high affinity (EC<sub>50</sub> = ~4.6 nM). The interaction of DR6-AP with full-length APP expressed in COS cells was also high affinity (half maximal saturation: ~1.3 nM) (Supplementary Fig. 8a, b). This binding was blocked by anti-N-APP(poly) (not shown) and anti-DR6.1 (Supplementary Fig. 8a) consistent with APP being a functional DR6 ligand.

Antibodies 4G8 and anti-sAPP $\beta$  used above are highly specific for APP. However, like other antibodies to the amino terminus of APP<sup>27</sup>, anti-APP(poly) also binds the close APP relative APLP2 (not shown). We found that a recombinant amino terminal fragment of APLP2 also binds DR6 (Supplementary Fig. 11a). Thus, APLP2 might contribute with APP to the bands

detected on Western by DR6-AP. Indeed, an antibody selective for the APLP2 amino terminus detected a shed fragment in conditioned medium after trophic deprivation (Supplementary Fig. 11b)). The relative contribution of APP and APLP2 fragments to DR6-AP binding sites remains to be determined.

To evaluate receptor specificity, we examined by pull-down the binding of APP[1–286] to ectodomains of the seven other death-domain containing members of the TNFR superfamily, and two orphan members. Only binding to p75NTR was observed (Supplementary Fig. 8d), suggesting that p75NTR may serve as an alternate route for APP effects in some settings; however, the affinity was considerably lower ( $EC_{50} = \sim 300$  nM by ELISA, Supplementary Fig. 8e). Consistent with DR6 being the major APP receptor, a fusion of APP[1–286] to alkaline phosphatase bound sensory axons in culture, but binding was significantly reduced by anti-DR6.1 or by using *DR6* knock-out neurons (Supplementary Fig. 12a, b); residual binding may represent background or binding to another receptor(s), possibly p75NTR.

### N-APP is necessary and sufficient for degeneration

To test whether the amino terminus of APP contributes to degeneration, we performed loss-of-function studies. Degeneration of sensory and commissural axons in response to trophic deprivation was inhibited by anti-N-APP(poly) (Fig. 5a, a', d, d'), which also inhibited death of sensory neuron cell bodies (Supplementary Fig. 13a, b), without affecting loss of surface APP following trophic deprivation (Supplementary Fig. 13c). Antibody 22C11<sup>28</sup> (Fig. 4h) also inhibited sensory axon degeneration (not shown). Because both antibodies also bind APLP2<sup>27</sup>, we performed a more selective blockade using RNA interference. Knock-down of APP in sensory neurons significantly impaired both axon degeneration and cell body death following trophic factor withdrawal (Fig. 5b, b'). These results support involvement of an amino-terminal fragment of APP in degeneration. In further support, BACE inhibitors impaired degeneration of sensory axons and cell bodies (Fig. 5c, c'; Supplementary Fig. 13a, b, 14) and commissural axons (Fig. 5d, d') following trophic deprivation. The selective BACE inhibitor AZ29 blocked degeneration at concentrations consistent with its cellular  $IC_{50}$  (470 nM<sup>26</sup>) (Supplementary Fig. 14a, a').

Importantly, axonal degeneration block by BACE inhibitors could be reversed by adding purified APP[1–286] to sensory (Fig. 5c, c') and commissural (Fig. 5d, d') neurons, showing that the amino terminus of APP is sufficient to trigger degeneration. This effect was blocked by anti-DR6.1 (Supplementary Fig. 14b, b'), consistent with DR6 being the major functional receptor in these cells. Block of sensory cell body degeneration by BACE inhibitors could likewise be reversed by addition of APP[1–286], albeit at higher concentrations (Supplementary Fig. 13a, b). Together, these results support the model that shed N-APP activates DR6 to trigger degeneration. Degeneration of sensory axons caused by APP[1–286] in presence of BACE inhibitor was blocked if NGF was present (50 ng/ml; Fig. 5c, c'), indicating that trophic factors inhibit signaling downstream of DR6.

### Physiological degeneration does not appear to involve Abeta toxicity

BACE cleavage of APP is followed by gamma secretase cleavage, yielding Abeta peptides<sup>19–22</sup> (Fig. 4h). Since Abeta peptides can be neurotoxic<sup>21,22</sup>, we examined whether they contribute to degeneration. Synthetic Abeta1–42 triggered degeneration in our assays, and an antibody directed to amino-acids 33–42 of Abeta (anti-Abeta[33–42]; Fig. 4h) blocked this effect (Supplementary Fig. 9a, e), but did not block degeneration following trophic deprivation (Fig. 5e, e'). Conversely, degeneration induced by synthetic Abeta was not blocked by genetic deletion of *DR6* (not shown), indicating that Abeta operates through a mode of action distinct from the physiological degeneration mechanism studied here.

Antibody 4G8 used above, which binds Abeta residues 17–24 (Fig. 4h), also blocked the degenerative effect of Abeta1–42 (Supplementary Fig. 9e), but unlike anti-Abeta[33–42], it partially inhibited degeneration following trophic deprivation (Fig. 5e, e'). However, as mentioned, 4G8 also partially inhibits loss of surface APP. In contrast, the APP epitope bound by anti-Abeta[33–42] is buried in the cell membrane, so anti-Abeta[33–42] does not bind intact APP nor inhibit its surface loss (Supplementary Fig. 9a, b, d). Since anti-Abeta[33–42] does not protect, we attribute the partial protective effect of 4G8 to its ability to inhibit APP shedding, not its ability to block Abeta toxicity. Since 4G8 does not bind APLP2, its ability to protect also supports the sufficiency of APP in mediating degeneration.

### ***In vivo* evidence for an APP-DR6 interaction**

To seek evidence of an APP/DR6 interaction *in vivo*, we examined whether the DR6 knock-out exhibits any phenotype similar to those reported in the APP knock-out – or, given the potential for redundancy, in compound mutants of APP with APLP2. One phenotype observed at the neuromuscular junction in the APP;APLP2 double knock-out is suggestive of a potential pruning defect. In wild-type animals, motor axons normally terminate at synaptic sites (Fig. 6a). In APP;APLP2 double knockouts, however, there is a highly penetrant presence of nerve terminals past end-plates<sup>29</sup>. Remarkably, a similar phenotype was observed in the DR6 mutant: rather than terminating at end-plates, many terminals were present beyond, giving characteristic finger-like protrusions (Fig. 6a, a'). It is not known whether this phenotype reflects failure to retract or excessive sprouting. Regardless, the similarity of phenotypes supports the view that APP signals via DR6 in regulating axonal behavior *in vivo*. In this system, APP and APLP2 appear redundant since the axonal phenotype is seen only in APP;APLP2 double mutants, not single mutants<sup>29</sup>. Whether they are non-redundant in other system remains to be determined.

## **Discussion**

Our results reveal a mechanism, the “APP/Death Receptor” mechanism (Fig. 6b), in which trophic deprivation leads to cleavage of surface APP by beta-secretase (BACE1), followed by further cleavage of the released fragment by an as yet unidentified mechanism (likely near the junction of APP acidic and “E2” domains) to yield an amino terminal ~35 kDa fragment (N-APP) which binds DR6, triggering caspase activation and degeneration of both neuronal cell bodies (via caspase-3) and axons (via caspase-6). Degeneration induced by added amino APP was blocked when trophic factor was present, indicating that trophic factors not only prevent initiation of the APP cleavage cascade, but also block signaling downstream of DR6, providing a fail-safe mechanism to protect if DR6 is inappropriately activated in an otherwise healthy neuron.

### **DR6: an accelerator of self-destruction**

In all settings examined, antagonizing DR6 resulted in a 24–48hr delay, rather than complete block, of neuron death and axonal pruning. DR6 is therefore best thought of as an accelerator of degeneration: neurons and axons activate it for swift self-destruction when they become atrophic, but without it they have other, slower, ways of achieving that end, perhaps involving other proapoptotic receptors<sup>5</sup> or intrinsic mechanisms. This function contrasts with that of the DR6 relative, p75NTR (which can mediate degeneration when overexpressed<sup>11</sup> or when activated by a neurotrophin in neurons lacking the cognate Trk receptor<sup>5</sup>). p75NTR is more restricted to specific neuronal classes than DR6, and its genetic deletion provided only modest protection of sensory axons in the first 36hr after trophic deprivation (Supplementary Fig. 15), as reported previously for sympathetic axons<sup>30</sup>. In sympathetic neurons, p75NTR is thought to mediate competition for NGF: cells with high NGF/TrkA signaling upregulate expression of BDNF, which acts via p75NTR to trigger degeneration of neighboring neurons with less

robust NGF/TrkA signaling<sup>30,31</sup>. This mechanism shares with ours expression of a prodegenerative ligand(s) by the neurons themselves. However, the DR6 ligand APP is activated by trophic factor *deprivation*, whereas p75NTR ligand expression is increased by trophic factor *stimulation*<sup>31</sup>. Thus, p75NTR ligands are released by “strong” neurons to kill “weak” neurons (a paracrine prodegenerative effect)<sup>31</sup>, whereas APP gets activated within “weak” neurons to accelerate self-destruction triggered by trophic deprivation or perhaps other insults (an autocrine prodegenerative effect)

### Caspase-6: an effector of axonal degeneration

The intracellular mechanisms of axonal degeneration and their relation to apoptosis have been unclear. Our results indicate that developmental axonal degeneration does involve an apoptotic pathway, but with a non-classical effector, caspase-6. Epistasis analysis supports a linear activation model from DR6 to Bax to caspase-6, but does not exclude that active caspase-6 might feed back, e.g. to accelerate the process; in this context, it is intriguing that the APP cytoplasmic domain is a caspase-6 substrate<sup>32</sup>. Activation of caspase-6 by trophic deprivation occurs in a punctate pattern in axons, leading to a “beads on a string” appearance, and sites of punctate caspase-6 activation correspond to sites of microtubule fragmentation. Caspase-6 might trigger microtubule destabilization by cleaving microtubule associated proteins like tau, a documented target of caspase-6<sup>33,34</sup>; in a recent proteomic analysis, almost half the identified caspase-6 targets were cytoskeleton-associated<sup>35</sup>.

### Ligands and receptors for self-destruction

Although p75NTR also binds APP[1–286], DR6 binds with much higher affinity, and blocking DR6 function largely blocks both APP[1–286] binding to sensory axons and degeneration triggered by APP[1–286]. Thus, DR6 appears to be the major functional APP receptor in these neurons, although p75NTR might contribute in other contexts. Conversely, APP may not be the only DR6 ligand: APLP2, which is coexpressed with APP in many neurons<sup>27</sup>, may also contribute to degeneration, since an amino terminal fragment is shed in response to trophic deprivation, can bind DR6, and can trigger degeneration when added exogenously (Supplementary Fig. 16). Future studies will define the relative contributions of APP and APLP2 in different neuronal populations.

The finding of similar neuromuscular junction phenotypes in *DR6* and *APP;APLP2* mutants supports a ligand-receptor interaction, and indicates that APP and APLP2 both contribute in this system. The aberrant axonal extensions seen could reflect an impairment of pruning, or, alternatively, a failure of axons to stop; of note, the APP ectodomain has been implicated in neurite growth inhibition<sup>36</sup>. Previous studies have not reported changes in neuronal cell death *in vivo* in *APP* mutants, either singly or in combination with *APLP1* and/or *APLP2* mutations<sup>37,38</sup>. However, such studies did not examine spinal cord or sensory ganglia, nor involve time course analysis to evaluate possible delays in degeneration. *In vitro* analysis of cortical neurons from mutants has given divergent results regarding their basal survival rates and susceptibility to glutamate excitotoxicity<sup>37–39</sup>, but their response to trophic deprivation has not been reported.

In recent findings paralleling ours, trophic deprivation was found to trigger BACE cleavage of APP in PC12 cell-derived neurons and primary hippocampal neurons, and degeneration was reduced by *APP* knock-down (in PC12 cells) and BACE inhibition<sup>40,41</sup>. The pro-degenerative function of APP was, however, attributed to Abeta, since antibodies to Abeta inhibited degeneration<sup>40,41</sup>. We too observed protection by antibody 4G8, but attribute this to 4G8’s ability to bind full-length APP and inhibit cleavage, since a different anti-Abeta antibody that does not bind native APP inhibited neither shedding nor physiological degeneration, but blocked the toxic action of added Abeta. Conversely, Abeta’s toxic effect was not blocked by



DR6 inhibition. It was also found that a gamma secretase inhibitor, which reduced Abeta production after BACE cleavage, inhibited degeneration<sup>40,41</sup>. We too found that gamma secretase inhibitors can partially inhibit degeneration of commissural and sensory axons (Supplementary Fig. 17), but gamma secretase has many substrates, and it is possible that efficient activation of DR6 signaling requires a distinct gamma secretase-dependent process. Thus, our results argue against involvement of Abeta in initiating DR6-dependent degeneration in neurons studied here, but this does not exclude its possible involvement in other neurons or at later times in these neurons to augment effects of APP/DR6 signaling.

### A role for APP/DR6 signaling in neurodegeneration

APP is expressed in adult brain and upregulated on damaged axons<sup>42</sup>. *DR6* is also highly expressed in adult brain (Supplementary Fig. 18). Given our findings, it is reasonable to assume that the APP/Death Receptor mechanism might contribute to adult plasticity, or to neurodegeneration following injury or in disease. Interestingly, *DR6* is upregulated in injured neurons<sup>43</sup>, raising the question whether overexpressed DR6 can trigger ligand-independent degeneration, as reported for p75NTR<sup>11</sup>.

Given the genetic evidence linking APP and its cleavage to Alzheimer's disease, we propose that this mechanism may in particular contribute to initiation or progression of Alzheimer's, either alone or in combination with other proposed APP-dependent mechanisms, such as Abeta toxicity<sup>24,25</sup> or effects of the APP intracellular domain<sup>44</sup>. Of note, (i) prior studies showed immunoreactivity for the APP amino terminus associated with Alzheimer's plaques<sup>45,46</sup>, (ii) *DR6* maps to chromosome 6p12.2-21.1, near a putative Alzheimer's Disease susceptibility locus<sup>47</sup>, and (iii) sites of *DR6* mRNA expression in adult brain correlate in an intriguing way with known sites of dysfunction in Alzheimer's: very high in hippocampus, high in cortex, but low in striatum (Supplementary Fig. 18), and high in forebrain cholinergic neurons<sup>48</sup>, for instance. In addition, activated caspase-6, a downstream DR6 effector, is associated with plaques and tangles in Alzheimer's disease, and with mild cognitive impairment<sup>34,49</sup>, consistent with possible activation of caspase-6 in neuritic processes by the APP/Death receptor mechanism (caspase-6 is also implicated in Huntington's disease<sup>50</sup>). While these results are compatible with involvement of APP/DR6 signaling in Alzheimer's, it is less clear how the mechanism fits with genetic evidence implicating altered gamma secretase processing in this disease<sup>19-22</sup>; however, the fact that gamma secretase inhibitors inhibit DR6-dependent degeneration hints at a possible relationship.

Thus, further study is required to elucidate the full implications of the APP/Death Receptor mechanism in development, adult physiology, and disease. Nonetheless, our results already tie APP to a novel mechanism for neuronal self-destruction in development, and suggest that the APP ectodomain, acting via DR6 and caspase-6, contributes to degeneration in Alzheimer's disease.

### Methods summary

Antibodies to the following targets were used: pro-caspase-3 (1:200; Upstate), active caspase-3 (1:200, R&D); pro-caspase-6 (1:200, Stratagene); active caspase-6 (1:100, BioVision); Tuj1 (1:500, Covance); p75NTR (Chemicon); 2H3 (1:200, DSHB); Islet1/2 (1:100; Santa Cruz Biotech); N-APP (polyclonal, 1:100, Thermo Fisher Scientific; monoclonal 22C11: Calbiochem); DR6 (R&D); NGF (Abcam and Genentech), BDNF (Calbiochem), and NT3 (Genentech); Abeta (4G8 (Covance), and "C-terminal cleavage-specific anti-Abeta antibody" (Anti-Abeta[33-42]) (Sigma)); and the C terminal cleavage site of sAPP $\beta$  (Covance). Monoclonal antibodies to human DR6 ectodomain fused with hFc (A.N., K. Dodge, V. Dixit, and M.T.L., in preparation), were screened for binding to murine DR6 and block of commissural neuron degeneration. Proteins used were: netrin-1 (R&D), NGF (Roche); BDNF

and NT3 (Calbiochem); control IgG (R&D). Transiently-expressed murine DR6 ectodomain (amino acids 1–349) fused to human Fc, His-tagged human APP[1–286], and APP[1–286] and APLP2[1–300] fused to human Fc, were affinity-purified from CHO cell supernatants (similar results were obtained with APP[1–286] and APP[1–306] (Novus Biologicals)). Inhibitors were used against: caspase-3 (Z-DEVD-FMK (Calbiochem)); caspase-6 (Z-VEID-FMK; BD Pharmingen); BACE (OM99-2 (Calbiochem); BACE Inhibitor IV (Calbiochem); AZ29 (Genentech)); gamma secretase (DAPT: Calbiochem).

See Methods for details of *in situ* hybridization and immunohistochemistry; explant, dissociated, and Campenot chamber cultures; siRNA transfection; tracing and quantitation of retinotectal projections; AP-binding assays; and pull-down assays.

## Methods

### *In situ* hybridization and immunochemistry

Radioactively labeled<sup>35</sup>S *in situ* mRNA hybridization was as described<sup>51</sup>, using the mRNA locator kit (Ambion). Radiolabeled mRNA probes to anti-sense sequences of mouse TNFR 3' UTRs were generated using the MAXIscript Kit (Ambion). Immunochemistry was as described on sections<sup>51</sup> or cultured cells<sup>52</sup>. Surface labeling was done without detergent. Double labeling was performed using Zenon Technology (Invitrogen). Fluorescent caspase reporter assays were as recommended (MP Biologicals). TUNEL assays was as recommended (*In Situ* Cell Death Detection Kit, Roche).

### Quantitation on sections

20 µm serial cryosections were taken from axially matched cervical (C1–C3) levels of *DR6* null embryos and heterozygous littermates. Caspase-3 positive cells were counted at E15.5 (12 mutants, 5 controls). Motoneurons were counted at E14.5 (large Islet1/2-positive ventral neurons; 7 mutants, 4 controls) or E18 (large H&E stained ventral neurons; 3 mutants, 3 controls).

### Neuronal cultures

E11.5 mouse or E13 rat dorsal spinal cord was dissected after introduction of plasmids and siRNAs by electroporation<sup>53</sup>; the dorsal explant survival assay was as described<sup>21</sup>. *DR6* siRNAs #1 and #2 (sense) were: 5'-CAAUAGGUCAGGAAGAUGGCU-3' and 5'-AAUCUGUUGAGUUCAUGCCUU-3'. The mismatch sequence complementary to #1 was: 5'-GGACTCTGTGTACAGTCACCTCCCAGATCTGTTATAG-3'. Sensory and motoneuron explants or dissociated cells were cultured on laminin-coated 35 mm tissue culture dishes in culture medium (Neurobasal medium with B27 supplement) with appropriate trophic factor (sensory: NGF, 50ug/ml; motor: BDNF and NT3, 10ug/ml). Trophic deprivation was achieved by removing growth factor and adding appropriate antibodies (sensory: anti-NGF, 50 ug/ml; motor: anti-BDNF and anti-NT3, 50 ug/ml). Introduction of siRNAs into dissociated sensory neuron cultures was performed as described<sup>54</sup>.

### Campenot Chamber assay

The Campenot Chamber assay was carried out as described<sup>22</sup> with minor modifications. Briefly, 35-mm tissue culture dishes were coated with PDL/Laminin and scratched with a pin rake (Tyler Research) to generate tracks, as illustrated in Fig. 2a. A drop of culture medium containing 4 mg/ml methylcellulose was placed on the scratched substratum. A teflon divider (Tyler Research) was seated on silicone grease and a dab of silicone grease was placed at the mouth of the center slot. Dissociated sensory neurons from E12.5 mouse DRGs were suspended in methylcellulose-thickened medium, loaded into a disposable sterile syringe fitted with a 22-

gauge needle, injected into center slot under a dissecting microscope, and allowed to settle overnight. The outer perimeter of the dish (the cell body compartment) and the inner axonal compartments were filled with methyl-cellulose-containing medium. Within 3–5 days *in vitro*, axons begin to emerge into left and right compartments. To trigger local axonal degeneration, NGF-containing medium from axonal compartments was replaced with neurobasal medium containing anti-NGF. Where indicated, anti-DR6.1 or control IgG were added (50 µg/ml final concentration) at the time of NGF deprivation. Cultures were fixed at different times following deprivation with 4% PFA for 30 min at room temperature (rt) and processed for TuJ1 immunofluorescence.

### Tracing of retinal ganglion cell axons

**Dil injection**—Injections of DiI into temporal retina and subsequent analyses were performed essentially as previously described<sup>55</sup>. The center of the TZ was determined to be the center of a circumscribed circle. The average center of the TZs was 50.3% for wild-types and 49.8% for mutants ( $p > 0.9$ ) from the medial edge. The retina in mutants appears morphologically normal with all retinal layers present in similar proportions to wild-type.

**Quantitative analysis**—The presence of axons was determined in 100µm vibratome sections and transposed onto the SC. Sections were photographed and axon presence recorded in 100µm segments from the anterior border. Using landmarks such as the TZ, unique arbors, or edge of the SC these data were transposed from photos of sections to photos of the wholemount SCs in dorsal view, resulting in a grid of 100µm squares covering each SC. The TZs and grids were aligned for the analyses.

### AP binding assays

The DR6 ectodomain fused to AP (DR6-AP) and APP[1–286] fused to AP (APP-AP) were transiently expressed in COS-1 cells. Medium was changed after 12hr to OPTI-MEM (Invitrogen), and conditioned-medium collected 36hrs later and filtered.

The DR6-AP blot assay on conditioned medium was performed as described<sup>56</sup>. Briefly, conditioned medium derived from sensory axons maintained in Campenot chambers or ventral spinal cord explants in explant culture (with or without trophic deprivation) was concentrated 10-fold using centrprep centrifugal filters (Millipore), resolved in 4–20% gels under non-reducing conditions, and blotted with DR6-AP in AP binding buffer.

For *in situ* sensory axon binding assays, wild-type or Bax null sensory explants were cultured, deprived of NGF for 12hr (with or without Bax inhibitor, as indicated), then washed twice with the AP binding buffer (HBSS, Gibco Cat. No. 14175-095, with 0.2% BSA, 0.1% NaN<sub>3</sub>, 5 mM CaCl<sub>2</sub>, 1 mM MgCl<sub>2</sub>, 20 mM HEPES, pH=7.0). The AP binding assay was carried out by making a 1:1 mixture of binding buffer and conditioned medium containing DR6-AP, APP-AP, or control AP, applied to DRG explants in 8-well culture slides and incubated 90 min at rt. Explants were rinsed five times with binding buffer, fixed with formaldehyde (3.7% in PBS) for 12 min at rt, and rinsed 3 times with HBS (20mM HEPES pH=7.0, 150 mM NaCl). Endogenous AP activity was blocked by heat inactivation at 65°C in HBS for 30 min. After rinsing three times in AP reaction buffer (100 mM TRIS pH=9.5, 100 mM NaCl, 50 mM MgCl<sub>2</sub>), bound AP fusion was visualized by developing color stain in AP reaction buffer with 1/50 (by volume) of NBT/BCIP stock solution (Roche) overnight at rt.

The *in situ* binding of DR6-AP to COS cells transiently expressing APP695 was performed in the same way, but with heparin (2–10 µg/ml) added to reduce non-specific binding. Transiently expressed p75NTR and DR6 expressed in COS-1 cells showed no specific binding under these conditions. For quantitative analysis, the amount of DR6-AP protein in medium was quantified

as described<sup>57</sup>. In brief, 100 microliters of 2xAP buffer (prepared by adding 100 mg Para-nitrophenyl phosphate (Sigma) and 15 ml of 1M MgCl<sub>2</sub> to 15ml 2M diethanolamine pH 9.8) was mixed with conditioned medium containing DR6-AP or control AP. The reaction was developed over 5–15 min, with the O.D. being in the linear range (0.1–1). The volume of reaction was adjusted by adding 800 microliters of distilled water, and O.D. measured at 405 nm absorbance. Concentration in nM was calculated according to the formula (for 100 ml): C (nM) = O.D. × 100 × (60/developing time)/30. Saturation binding analysis was performed as described<sup>57</sup>. Prizm 4 software (GraphPad) was used to generate saturation binding curves and to determine half-maximal saturation value.

### APP pull-down assays

Soluble ectodomains of TNFR superfamily members fused to human Fc were expressed in CHO cells and affinity purified. They were incubated at 5 ug/ml in binding buffer (HBSS, Gibco Cat. No. 14175-095, with 0.2% BSA, 0.1% NaN<sub>3</sub>, 5 mM CaCl<sub>2</sub>, 1 mM MgCl<sub>2</sub>, 20 mM HEPES, pH=7.0) with 1 ug/ml of His-tagged APP[1–286] and protein A/G beads (Santa Cruz Bio) at 4°C overnight. Beads were washed five times with binding buffer. Bound complexes were eluted from beads with SDS loading buffer, resolved in 4–20% SDS PAGE gels, and blotted for APP (with anti-NAPP(poly)) and for TNFR family members (with anti-hFc).

### Mice

The following mutant mice were used: *DR6* knock-out<sup>17</sup> (gift of Dr. V, Dixit); *Bax* knock-out<sup>58</sup> (gift of Dr. S. Korsmeyer); *p75NTR* knock-out<sup>59</sup> (Jackson laboratory).

### Supplementary Material

Refer to Web version on PubMed Central for supplementary material.

### Acknowledgments

We thank Richard Axel, Cori Bargmann, Vishva Dixit, Joe Lewcock, Richard Scheller, Bob Vassar, Ryan Watts, and members of the Tessier-Lavigne laboratory, for helpful discussions and suggestions, and critical reading of the manuscript, and Allison Bruce for making the diagrams. We thank Phil Hass and members of his laboratory (Genentech) for generation and purification of the DR6 ectodomain and APP[1–286], and Wei-Ching Liang and Yan Wu for binding experiments with purified proteins.

### References

1. Raff MC, Whitmore AV, Finn JT. Axonal self-destruction and neurodegeneration. *Science* 2002;296:868–71. [PubMed: 11988563]
2. Luo L, O'Leary DD. Axon retraction and degeneration in development and disease. *Annu Rev Neurosci* 2005;28:127–56. [PubMed: 16022592]
3. Buss RR, Sun W, Oppenheim RW. Adaptive roles of programmed cell death during nervous system development. *Annu Rev Neurosci* 2006;29:1–35. [PubMed: 16776578]
4. Saxena S, Caroni P. Mechanisms of axon degeneration: from development to disease. *Prog Neurobiol* 2007;83:174–91. [PubMed: 17822833]
5. Haase G, Pettmann B, Raoul C, Henderson CE. Signaling by death receptors in the nervous system. *Curr Opin Neurobiol*. 2008
6. Kuida K, et al. Decreased apoptosis in the brain and premature lethality in CPP32-deficient mice. *Nature* 1996;384:368–72. [PubMed: 8934524]
7. White FA, Keller-Peck CR, Knudson CM, Korsmeyer SJ, Snider WD. Widespread elimination of naturally occurring neuronal death in *Bax*-deficient mice. *J Neurosci* 1998;18:1428–39. [PubMed: 9454852]

8. Finn JT, et al. Evidence that Wallerian degeneration and localized axon degeneration induced by local neurotrophin deprivation do not involve caspases. *J Neurosci* 2000;20:1333–41. [PubMed: 10662823]
9. Kuo CT, Zhu S, Younger S, Jan LY, Jan YN. Identification of E2/E3 ubiquitinating enzymes and caspase activity regulating *Drosophila* sensory neuron dendrite pruning. *Neuron* 2006;51:283–90. [PubMed: 16880123]
10. Williams DW, Kondo S, Krzyzanowska A, Hiromi Y, Truman JW. Local caspase activity directs engulfment of dendrites during pruning. *Nat Neurosci* 2006;9:1234–6. [PubMed: 16980964]
11. Plachta N, et al. Identification of a lectin causing the degeneration of neuronal processes using engineered embryonic stem cells. *Nat Neurosci* 2007;10:712–9. [PubMed: 17486104]
12. Sagot Y, et al. Bcl-2 overexpression prevents motoneuron cell body loss but not axonal degeneration in a mouse model of a neurodegenerative disease. *J Neurosci* 1995;15:7727–33. [PubMed: 7472523]
13. Watts RJ, Hoopfer ED, Luo L. Axon pruning during *Drosophila* metamorphosis: evidence for local degeneration and requirement of the ubiquitin-proteasome system. *Neuron* 2003;38:871–85. [PubMed: 12818174]
14. Bodmer JL, Schneider P, Tschoep J. The molecular architecture of the TNF superfamily. *Trends Biochem Sci* 2002;27:19–26. [PubMed: 11796220]
15. Bossen C, et al. Interactions of tumor necrosis factor (TNF) and TNF receptor family members in the mouse and human. *J Biol Chem* 2006;281:13964–71. [PubMed: 16547002]
16. Pan G, et al. Identification and functional characterization of DR6, a novel death domain-containing TNF receptor. *FEBS Lett* 1998;431:351–6. [PubMed: 9714541]
17. Zhao H, et al. Impaired c-Jun amino terminal kinase activity and T cell differentiation in death receptor 6-deficient mice. *J Exp Med* 2001;194:1441–8. [PubMed: 11714751]
18. Schmidt CS, et al. Enhanced B cell expansion, survival, and humoral responses by targeting death receptor 6. *J Exp Med* 2003;197:51–62. [PubMed: 12515813]
19. Walsh DM, et al. The APP family of proteins: similarities and differences. *Biochem Soc Trans* 2007;35:416–20. [PubMed: 17371289]
20. Reinhard C, Hebert SS, De Strooper B. The amyloid-beta precursor protein: integrating structure with biological function. *Embo J* 2005;24:3996–4006. [PubMed: 16252002]
21. Hardy J, Selkoe DJ. The amyloid hypothesis of Alzheimer's disease: progress and problems on the road to therapeutics. *Science* 2002;297:353–6. [PubMed: 12130773]
22. Haass C, Selkoe DJ. Soluble protein oligomers in neurodegeneration: lessons from the Alzheimer's amyloid beta-peptide. *Nat Rev Mol Cell Biol* 2007;8:101–12. [PubMed: 17245412]
23. Wang H, Tessier-Lavigne M. En passant neurotrophic action of an intermediate axonal target in the developing mammalian CNS. *Nature* 1999;401:765–9. [PubMed: 10548102]
24. Campenot RB, Walji AH, Draker DD. Effects of sphingosine, staurosporine, and phorbol ester on neurites of rat sympathetic neurons growing in compartmented cultures. *J Neurosci* 1991;11:1126–39. [PubMed: 2010808]
25. Cole SL, Vassar R. BACE1 structure and function in health and Alzheimer's disease. *Curr Alzheimer Res* 2008;5:100–20. [PubMed: 18393796]
26. Edwards PD, et al. Application of fragment-based lead generation to the discovery of novel, cyclic amidine beta-secretase inhibitors with nanomolar potency, cellular activity, and high ligand efficiency. *J Med Chem* 2007;50:5912–25. [PubMed: 17985862]
27. Slunt HH, et al. Expression of a ubiquitous, cross-reactive homologue of the mouse beta-amyloid precursor protein (APP). *J Biol Chem* 1994;269:2637–44. [PubMed: 8300594]
28. Hilbich C, Monning U, Grund C, Masters CL, Beyreuther K. Amyloid-like properties of peptides flanking the epitope of amyloid precursor protein-specific monoclonal antibody 22C11. *J Biol Chem* 1993;268:26571–7. [PubMed: 7504673]
29. Wang P, et al. Defective neuromuscular synapses in mice lacking amyloid precursor protein (APP) and APP-Like protein 2. *J Neurosci* 2005;25:1219–25. [PubMed: 15689559]
30. Singh KK, et al. Developmental axon pruning mediated by BDNF-p75NTR-dependent axon degeneration. *Nat Neurosci*. 2008
31. Deppmann CD, et al. A model for neuronal competition during development. *Science* 2008;320:369–73. [PubMed: 18323418]

32. LeBlanc A, Liu H, Goodyer C, Bergeron C, Hammond J. Caspase-6 role in apoptosis of human neurons, amyloidogenesis, and Alzheimer's disease. *J Biol Chem* 1999;274:23426–36. [PubMed: 10438520]
33. Horowitz PM, et al. Early N-terminal changes and caspase-6 cleavage of tau in Alzheimer's disease. *J Neurosci* 2004;24:7895–902. [PubMed: 15356202]
34. Guo H, et al. Active caspase-6 and caspase-6-cleaved tau in neuropil threads, neuritic plaques, and neurofibrillary tangles of Alzheimer's disease. *Am J Pathol* 2004;165:523–31. [PubMed: 15277226]
35. Klaiman G, Petzke TL, Hammond J, Leblanc AC. Targets of caspase-6 activity in human neurons and Alzheimer disease. *Mol Cell Proteomics* 2008;7:1541–55. [PubMed: 18487604]
36. Young-Pearse TL, Chen AC, Chang R, Marquez C, Selkoe DJ. Secreted APP regulates the function of full-length APP in neurite outgrowth through interaction with integrin beta1. *Neural Develop* 2008;3:15.
37. Heber S, et al. Mice with combined gene knock-outs reveal essential and partially redundant functions of amyloid precursor protein family members. *J Neurosci* 2000;20:7951–63. [PubMed: 11050115]
38. Perez RG, Zheng H, Van der Ploeg LH, Koo EH. The beta-amyloid precursor protein of Alzheimer's disease enhances neuron viability and modulates neuronal polarity. *J Neurosci* 1997;17:9407–14. [PubMed: 9390996]
39. Han P, et al. Suppression of cyclin-dependent kinase 5 activation by amyloid precursor protein: a novel excitoprotective mechanism involving modulation of tau phosphorylation. *J Neurosci* 2005;25:11542–52. [PubMed: 16354912]
40. Matrone C, et al. Activation of the amyloidogenic route by NGF deprivation induces apoptotic death in PC12 cells. *J Alzheimers Dis* 2008;13:81–96. [PubMed: 18334760]
41. Matrone C, Ciotti MT, Mercanti D, Marolda R, Calissano P. NGF and BDNF signaling control amyloidogenic route and Aβ production in hippocampal neurons. *Proc Natl Acad Sci U S A* 2008;105:13139–44. [PubMed: 18728191]
42. Medana IM, Esiri MM. Axonal damage: a key predictor of outcome in human CNS diseases. *Brain* 2003;126:515–30. [PubMed: 12566274]
43. Chiang LW, et al. An orchestrated gene expression component of neuronal programmed cell death revealed by cDNA array analysis. *Proc Natl Acad Sci U S A* 2001;98:2814–9. [PubMed: 11226323]
44. Muller T, Meyer HE, Egensperger R, Marcus K. The amyloid precursor protein intracellular domain (AICD) as modulator of gene expression, apoptosis, and cytoskeletal dynamics—relevance for Alzheimer's disease. *Prog Neurobiol* 2008;85:393–406. [PubMed: 18603345]
45. Van Gool D, De Strooper B, Van Leuven F, Dom R. Amyloid precursor protein accumulation in Lewy body dementia and Alzheimer's disease. *Dementia* 1995;6:63–8. [PubMed: 7606281]
46. Palmert MR, et al. Antisera to an amino-terminal peptide detect the amyloid protein precursor of Alzheimer's disease and recognize senile plaques. *Biochem Biophys Res Commun* 1988;156:432–7. [PubMed: 3140814]
47. Bertram L, Tanzi RE. Alzheimer's disease: one disorder, too many genes? *Hum Mol Genet* 2004;13 (Spec No 1):R135–41. [PubMed: 14764623]
48. Doyle JP, et al. Application of a translational profiling approach for the comparative analysis of CNS cell types. *Cell* 2008;135:749–62. [PubMed: 19013282]
49. Albrecht S, et al. Activation of caspase-6 in aging and mild cognitive impairment. *Am J Pathol* 2007;170:1200–9. [PubMed: 17392160]
50. Graham RK, et al. Cleavage at the caspase-6 site is required for neuronal dysfunction and degeneration due to mutant huntingtin. *Cell* 2006;125:1179–91. [PubMed: 16777606]
51. Sabatier C, et al. The divergent Robo family protein rig-1/Robo3 is a negative regulator of slit responsiveness required for midline crossing by commissural axons. *Cell* 2004;117:157–69. [PubMed: 15084255]
52. Atwal JK, et al. PirB is a functional receptor for myelin inhibitors of axonal regeneration. *Science* 2008;322:967–70. [PubMed: 18988857]
53. Chen Z, et al. Alternative Splicing of the Robo3 Axon Guidance Receptor Governs the Midline Switch. *Neuron* 2008 May 8;58(3):325–32. [PubMed: 18466743]

54. Higuchi H, Yamashita T, Yoshikawa H, Tohyama M. Functional inhibition of the p75 receptor using a small interfering RNA. *Biochem Biophys Res Commun* 2003;301:804–9. [PubMed: 12565852]
55. McLaughlin T, Torborg CL, Feller MB, O'Leary DD. Retinotopic map refinement requires spontaneous retinal waves during a brief critical period of development. *Neuron* 2003;40:1147–60. [PubMed: 14687549]
56. Pettmann B, et al. Biological activities of nerve growth factor bound to nitrocellulose paper by Western blotting. *J Neurosci* 1988;8:3624–32. [PubMed: 3193174]
57. Okada A, et al. Boc is a receptor for sonic hedgehog in the guidance of commissural axons. *Nature* 2006;444:369–73. [PubMed: 17086203]
58. Knudson CM, et al. Bax-deficient mice with lymphoid hyperplasia and male germ cell death. *Science* 1995;270:96–99. [PubMed: 7569956]
59. Lee KF, et al. Targeted mutation of the gene encoding the low affinity NGF receptor p75 leads to deficits in the peripheral sensory nervous system. *Cell* 1992;69:737–749. [PubMed: 1317267]

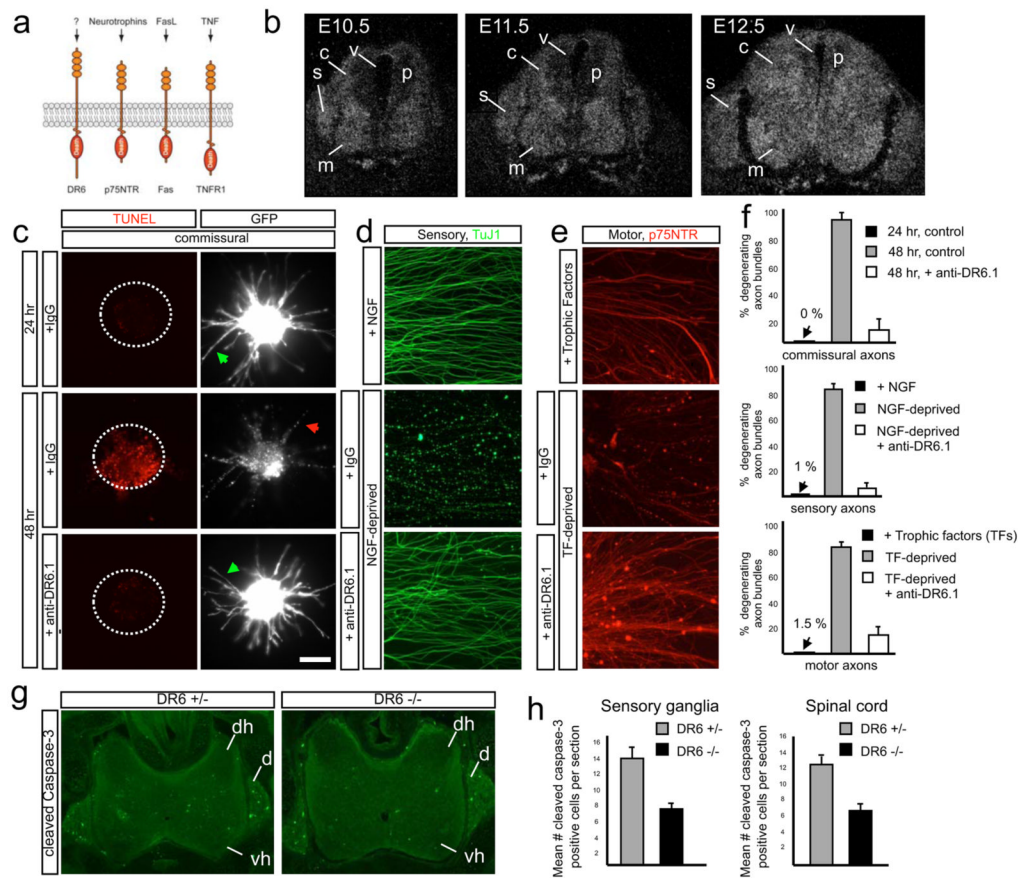


**Fig. 1. DR6 regulates degeneration of multiple neuronal classes**

(a) Diagram of several TNFR superfamily members possessing Death Domains. (b) *DR6* mRNA is expressed by differentiating spinal neurons (including motor (m) and commissural (c)), and by sensory neurons (s) in DRG at E10.5 – E12.5. Expression is low in neuronal progenitors (p) in the ventricular zone (v). (c–f) Anti-DR6.1 (50ug/ml) reduces degeneration *in vitro*, (c) Anti-DR6.1 inhibits commissural axon degeneration (visualized with GFP, right) and cell body death (TUNEL labeling, left; dots indicate explants) seen after 48hr in dorsal spinal cord cultures, (d, e) Effect on degeneration of sensory (d) or motor (e) axons triggered by trophic deprivation. Axons visualized by immunostaining for tubulin (TuJ1; sensory) or p75NTR (motor), (f) Percent degenerating axon bundles in (c–e) (mean  $\pm$  S.E.M.). (g, h) Genetic ablation of *DR6* decreases apoptosis *in vivo*. (g) Immunohistochemistry for cleaved caspase-3 in cervical spinal cord (dh, dorsal horn; vh, ventral horn) and DRG (d) of E15.5 *DR6* mutants and heterozygous littermates. (h) Number of positive cells per serial 20  $\mu$ m section (mean  $\pm$  S.E.M.). Scale bar, (c, d): 50  $\mu$ m; (e): 50  $\mu$ m; (g, h): 110  $\mu$ m.



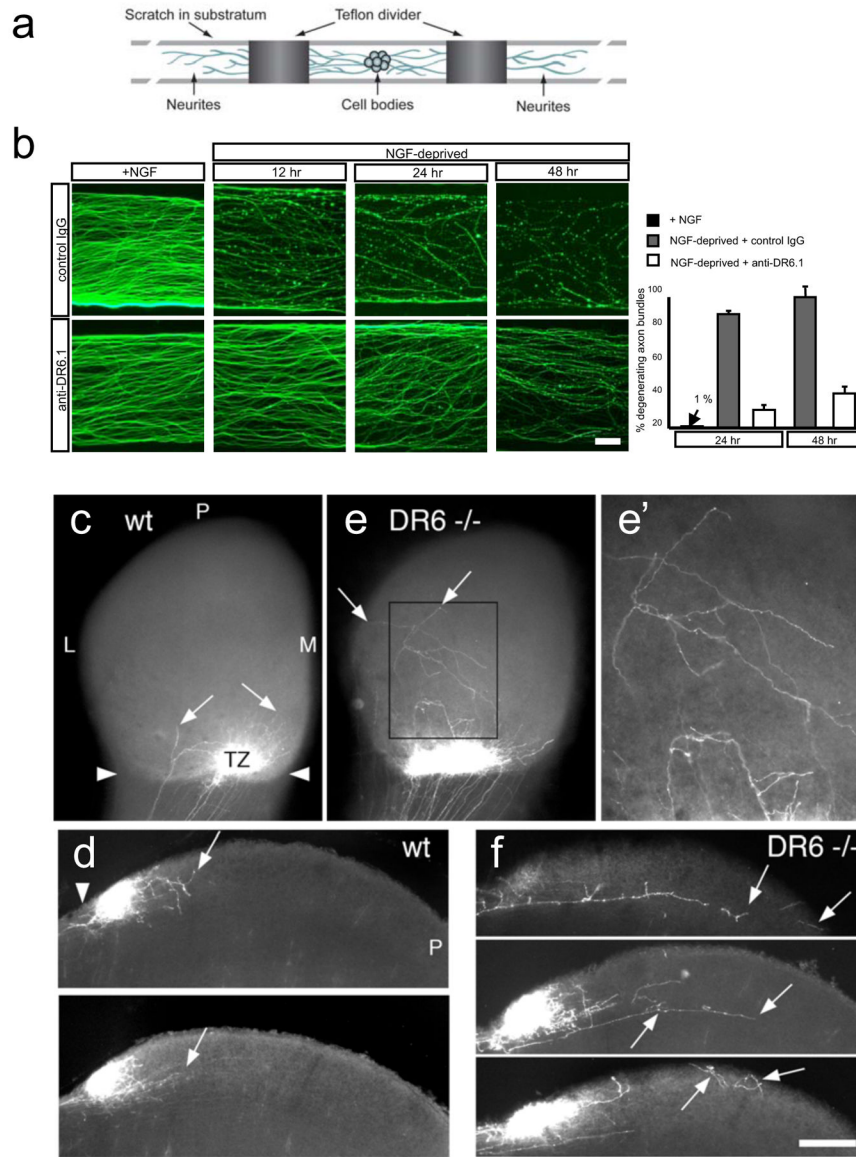


**Figure 2. DR6 regulates axon pruning *in vitro* and *in vivo***

**(a)** Diagram of Campenot chamber (adapted from ref. (24)).

**(b)** Local degeneration of sensory axons (TuJ1 immunostain) in Campenot chambers after NGF deprivation from the axonal compartment (top) was delayed by anti-DR6.1 (50 ug/ml) added at time of deprivation (bottom). Right: percent degenerating bundles at 24 and 48hr.

**(c–j)** Compromised pruning of retinal axons in *DR6*<sup>-/-</sup> mice. Dorsal view of **(c, e)**, and vibratome sections through **(d, f)**, the superior colliculus (SC) of wt **(c, d)** or *DR6*<sup>-/-</sup> **(e, f)** mice at P6. **(c, d)** In wild-type, diI-labeled temporal retinal ganglion cell (RGC) axons form a dense termination zone (TZ) in anterior SC (arrowheads: anterior border). Few are outside the immediate TZ area (arrows), **(e, f)** In *DR6*<sup>-/-</sup> mice, temporal RGC axons and arbors are present in areas far from the TZ (inset, magnified in **(e')**) and well posterior to it (arrows). P: posterior; L, lateral; M, medial.

Scale bar: **(b)**: 200 μm; 400 μm **(c, e)**; 170 μm **(e')**; 250 μm **(d, f)**.

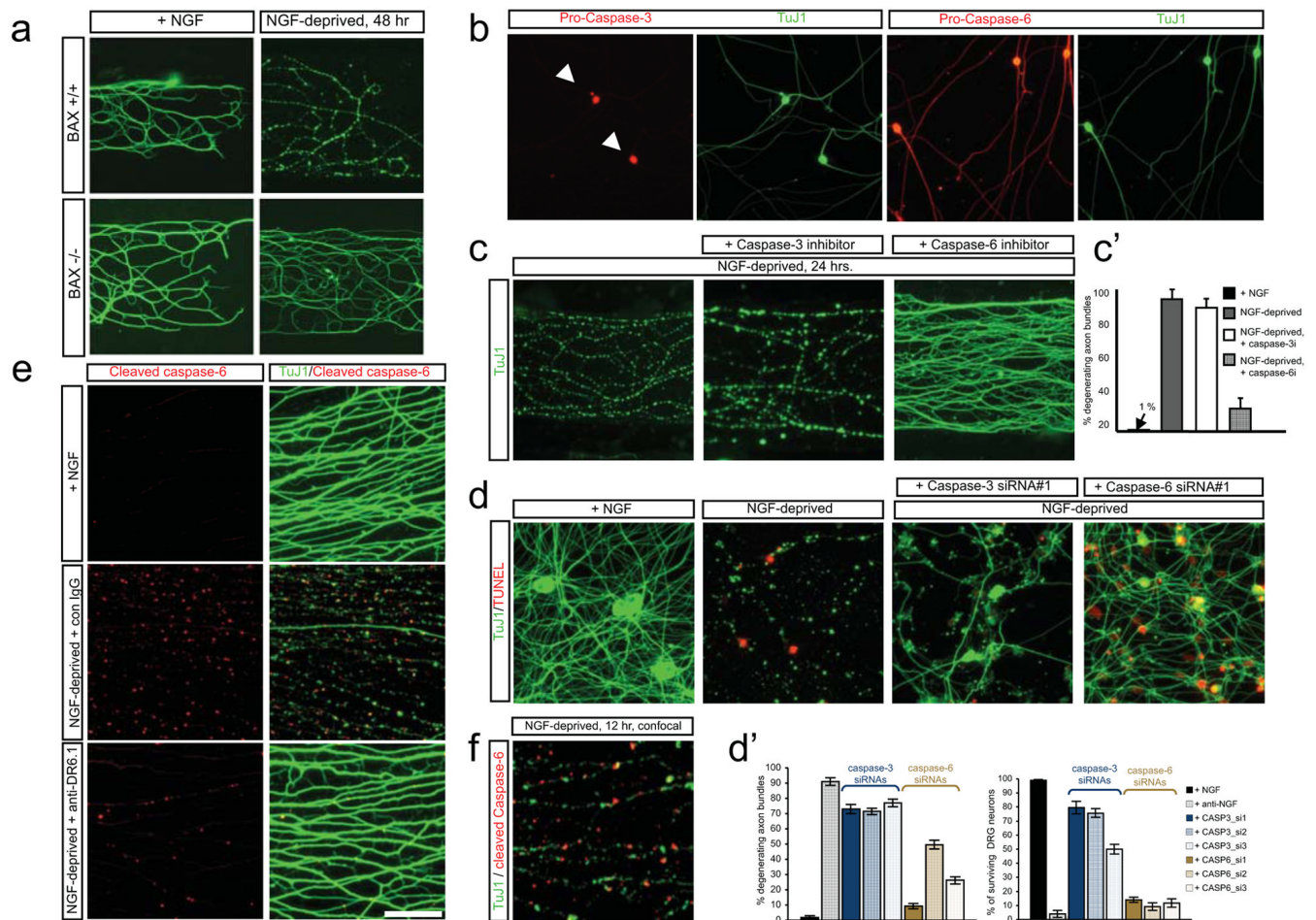


### Figure 3. Bax and Caspase-6 regulate axonal degeneration

(a) Local sensory axon degeneration (TuJ1 immunostain) 48hr after NGF deprivation in Camponot chambers was blocked in neurons from *Bax*<sup>-/-</sup> mice.

(b) Dissociated sensory neurons double-labeled for pro-caspase-3 and TuJ1 (left), or pro-caspase-6 and TuJ1 (right). Caspase-3 is detected in cell bodies (arrowheads), caspase-6 in both cell bodies and axons.

(c) Local degeneration of sensory axons in Camponot chambers deprived of NGF for 24hr is inhibited by a caspase-6 inhibitor (zVEID-FMK) but not a caspase-3/7 inhibitor (zDEVD-FMK). Quantification in (c').

(d) In dissociated sensory neuron cultures deprived of NGF for 24hr, siRNA knock-down of *caspase-3* primarily rescues cell body death (TUNEL label), whereas *caspase-6* knock-down primarily rescues axonal degeneration. Quantification in (d'). Extent of inhibition by individual siRNAs correlates with degree of target knock-down (Supplementary Fig. 6d).

(e) Detection of caspase-6 activation in sensory axons with a cleaved caspase-6-specific antibody (left; TuJ1 double-label on right). Punctate activation of caspase-6 following NGF deprivation (16 hr, middle) was reduced by anti-DR6.1 (bottom).

(f) Confocal section of a field from (e) shows that activated caspase-6 puncta correspond to sites of tubulin loss (fraction non-overlapping: 79 ± 5%).

Scale bar: (a), 250 μm (b): 100 μm; (c): 90 μm; (d): 75 μm; (g): 50 μm; (h): 25 μm.

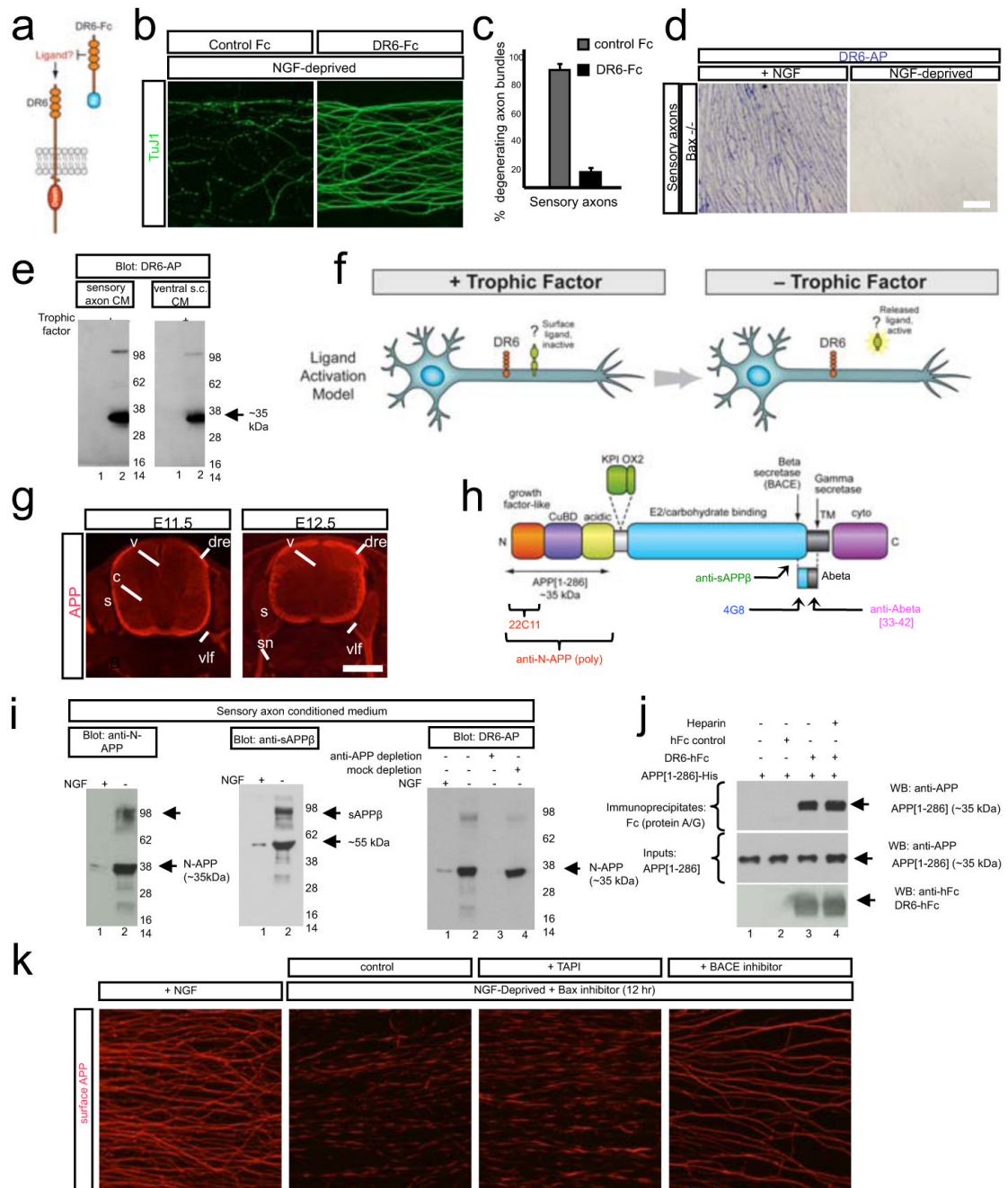


#### Figure 4. The amino terminus of APP is a regulated DR6 ligand

(a) Hypothesis: if DR6 is ligand-activated, then DR6-Fc might sequester the ligand and inhibit degeneration.

(b) DR6-Fc inhibits local degeneration of sensory axons in Campenot chambers 24hr after NGF deprivation. Quantification in (c).

(d, e) DR6-binding sites are lost from axons and released into medium upon trophic deprivation. (d) DR6-AP binding (purple) to Bax<sup>-/-</sup> sensory axons (left) is lost 24hr after NGF deprivation (right), (e) Medium conditioned by sensory axons (in Campenot chambers) or ventral spinal cord explants, maintained with or deprived of trophic factors for 24 hr (sensory:

NGF; motor: BDNF and NT3; Bax inhibitor present), was resolved under non-reducing conditions and probed with DR6-AP.

**(f)** Results in **(a–e)** support a “Ligand Activation” model in which an inactive DR6 surface ligand is shed in active form upon trophic deprivation.

**(g)** APP immunostaining on sections of mouse embryos at indicated ages, showing neuronal and axonal expression, v, ventricular zone; drez, dorsal root entry zone; vlf, ventro-lateral funiculus; s, sensory ganglia; sn, spinal nerve.

**(h)** Domain structure of APP (short form, APP695), indicating beta- and gamma-secretase cleavage sites and antibody binding sites. KPI and OX2: alternatively spliced domains of longer form. Adapted from ref. (20).

**(i)** DR6 binding sites in sensory axon conditioned medium include APP ectodomain fragments. Left: anti-N-APP(poly) detects bands at ~35 kDa (N-APP, major) and ~100 kDa (minor), enriched after trophic deprivation. Middle: anti-sAPP $\beta$  detects bands at ~55kDa (major) and ~100 kDa minor). Right: Immunodepletion using anti-N-APP(poly) depletes DR6-AP binding sites.

**(j)** Direct interaction between purified APP [1–286] and DR6-Fc revealed by pull-down.

**(k)** Loss of surface APP in patches from sensory axons 12hr after NGF deprivation is blocked by the BACE inhibitor OM99-2 (10 $\mu$ M) but not the alpha-secretase inhibitor TAPI (20 $\mu$ M).

Scale bar: **(b)**: 50  $\mu$ m; **(d)**: 50  $\mu$ m; **(g)**: 500  $\mu$ m; **(i)** 50  $\mu$ m.

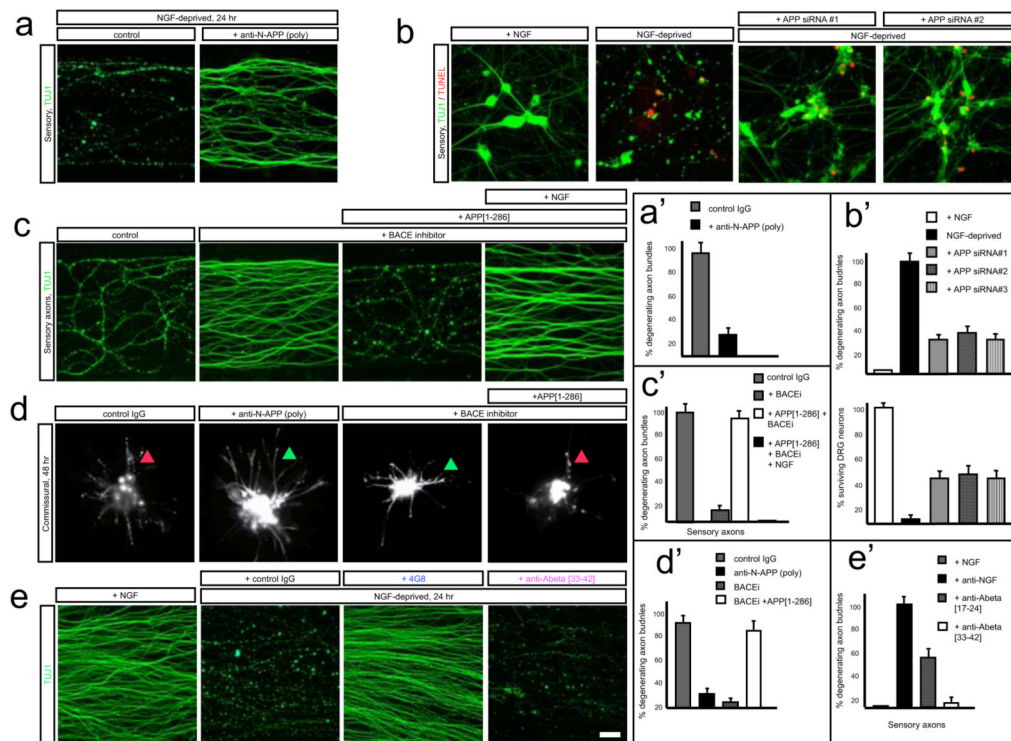


### Figure 5. The APP amino terminus regulates degeneration

(a) Local degeneration of sensory axons in Campenot chambers (NGF deprivation, 24hr) was blocked by anti-N-APP(poly) (20 ug/ml). Quantification in (a').

(b) In dissociated sensory neurons, siRNA knock-down of *APP* significantly reduces axon degeneration 24hr after trophic deprivation, and partially reduces cell body death. Quantification in (b').

(c) Local degeneration of sensory axons in Campenot chambers (NGF deprivation, 24hr) was inhibited by local addition of BACE inhibitor OM99-2 (10 $\mu$ M). Purified APP[1–286] added locally restored axonal degeneration, an effect inhibited by 50 ng/ml NGF (right). Quantification in (c').

(d) Degeneration of commissural neurons and axons at 48hr was inhibited by anti-N-APP(poly) (20 ug/ml) or BACE inhibitor OM99-2 (10 $\mu$ M), but restored by APP[1–286]. Quantification in (d').

(e) Effect of Abeta antibodies on sensory axon degeneration (NGF deprivation, 24hr). 4G8 partially inhibited; anti- Abeta[17–24] did not. Quantification in (e').

Scale bar: (a, c, e): 50  $\mu$ m; (b): 40  $\mu$ m; (d): 200  $\mu$ m.

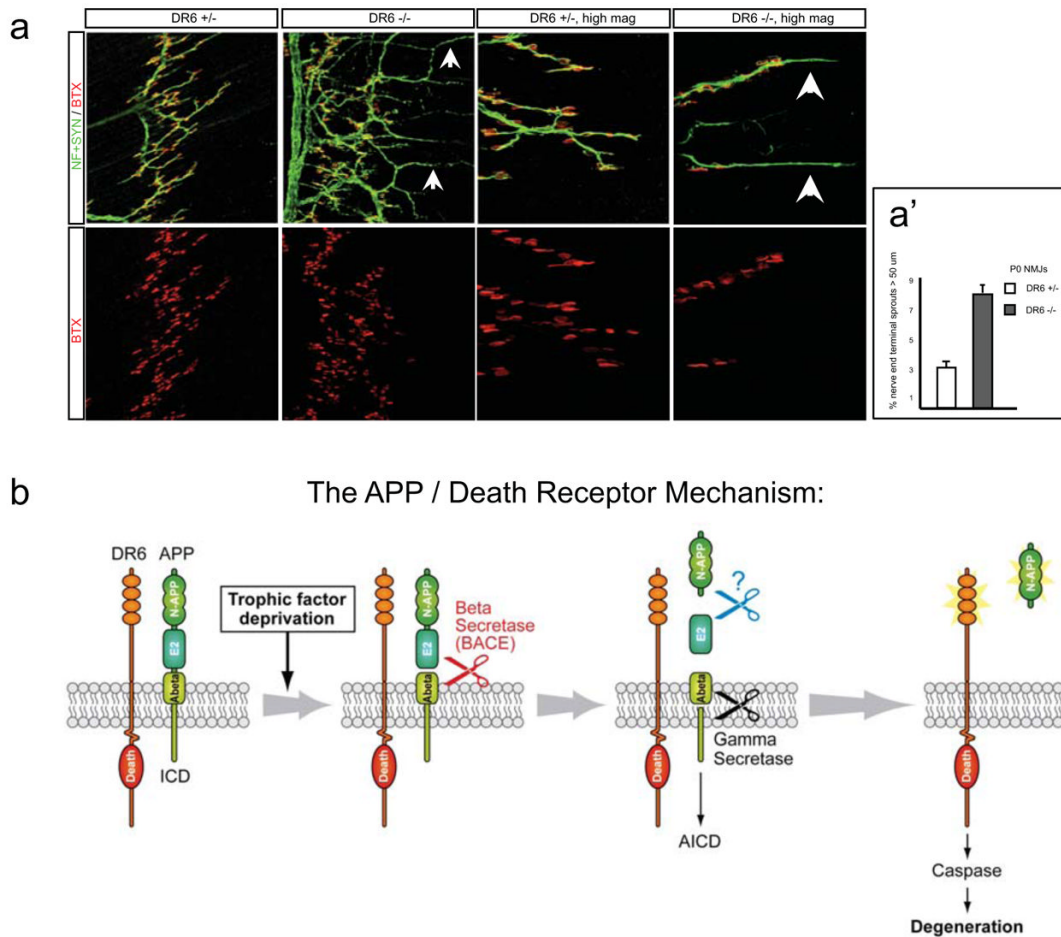


**Figure 6. APP/DR6 signaling: *in vivo* evidence, and model**

(a) In control (*DR6*<sup>+/-</sup>) P0 diaphragm muscle, few axons (green, neurofilament and synaptophysin stain) overshoot endplates (red, fluorescent alpha-bungarotoxin stain), and those that do are short, but in *DR6* mutants more overshoot and many are long (arrowheads), (a') Number overshooting by > 50 μm (this underestimates the effect, since overshooting axons are longer in mutants). Scale bar: 60 μm (left panels), 15 μm (right).

(b) The “APP/Death Receptor” mechanism. Trophic deprivation triggers cleavage of surface APP by BACE1, releasing sAPPβ, which is further cleaved by an unknown mechanism (“?”) to release N-APP, which binds DR6 to trigger degeneration through caspase-6 in axons and caspase-3 in cell bodies. Also illustrated is cleavage by gamma secretase to release Abeta and the APP intracellular domain (AICD).